Causes of anomalous solid formation in the exhaust systems of low-pressure chemical vapor deposition and plasma enhanced chemical vapor deposition semiconductor processes

Raul A. Abreu and Alan P. Troup
Edwards High Vacuum International, Manor Royal, Crawley RH10 2LW, United Kingdom

Michael K. Sahm
The BOC Group Technical Center, Murray Hill, New Jersey 07974

(Received 15 November 1993; accepted 7 March 1994)

The waste gases in low-pressure chemical vapor deposition and plasma enhanced chemical vapor deposition semiconductor processes react strongly with residual air in the exhaust of the vacuum pump to form solid deposits. It is common practice to purge the exhaust line with pure nitrogen to reduce the concentration of ambient air between the pump and the scrubber to an acceptable low level. However, the unexpected high quantities of exhaust deposits found in some systems cannot be explained by air leaks, impurities in the nitrogen, or diffusion. The problem of anomalous exhaust deposit formation was examined experimentally. A 40 mm pipe, up to 5 m in length and initially filled with nitrogen, was connected to an 80 m^3/h dry vacuum pump exhausting to air at atmospheric pressure. The composition of the atmosphere in the pipe was analyzed with a mass spectrometer. Under static conditions, the gas density distribution was ultimately limited, as expected, by simple interdiffusion. When the pump was running, however, there was a dramatic enhancement of the oxygen concentration throughout the pipe. The experimental observations were interpreted in terms of Richardson's annular effect. It is shown that the pressure fluctuations typical of vacuum pumps are responsible for the enhanced counterflow of air. The effect can be reduced by applying nitrogen purge but, even with a moderate 20 ℓ/min flow rate, deposits can form due to air transported back from the scrubber or exhaust duct.

I. INTRODUCTION

In the semiconductor industry, chemical vapor deposition is a preferred technique when dielectric layers of SiO_2 or Si_3N_4 are to be deposited onto silicon wafers as part of the circuit-building process. Silicon-containing gases such as silane (SiH_4), disilane (Si_2H_6) and dichlorosilane (SiH_2Cl_2) are commonly used. The reactors are held at moderately low pressure (of order 1 mbar) to prevent the gas-phase formation of particles. Typical process flow rates of silane or dichlorosilane are of order 0.05–0.5 sℓ/min (sℓ=standard liters) and a high throughput reactor may require a feed of order 8 moles of silicon-containing gas per day. In all cases, the surface reaction consumes only a fraction (often less than 30%) of the silicon-containing gas in the film deposition process; the remainder is quickly removed by a vacuum pump in order to minimize unwanted deposition on the walls of the reactor. Once well clear of the reactor and while still at low pressure, the chemical reaction slows enormously and there is little deposition in the vacuum foreline. Nitrogen is added at several stages of the compression process in order to dilute the local gas mixture below the lower explosion limit (LEL). Upon exiting the pump, the exhaust mixture typically flows through several meters of stainless-steel pipe which communicates either with a local wet scrubber or with the main exhaust duct, where the gas mixture is finally scrubbed before exhausting to the atmosphere.

The exhaust gases remain very reactive: a typical 10:1 mixture of ammonia and dichlorosilane will react spontaneously at room temperature and at any pressure above 30 mbar to produce the characteristic grey deposits normally found in low-pressure chemical vapor deposition (LPCVD) nitride process pumps. The unused silicon-containing waste gas can also react with residual oxygen or water vapor, resulting in oxides of silicon which manifest as very hard, white deposits [silane and oxygen have been shown to burn spontaneously at partial pressures as low as 0.27 mbar (Ref. 1)]. Oxides are very abrasive if present in a mechanism and are difficult to remove once coated onto metal surfaces. It is therefore essential to eliminate all sources of oxygen or water vapor from exhaust lines if system reliability is not to be severely compromised.

In the semiconductor industry, it is commonly believed that the only significant source of oxygen contamination is from air leaks into the subatmospheric part of the system and checks are made accordingly for leaks greater than 10^{-5} mbar ℓ/s before running a process. Flows of nitrogen gas, in excess of 10 ℓ/min, are introduced in the reasonable belief that downstream air in the exhaust system will be unable to migrate back toward the pump against the nitrogen flow. Even in leak-tight systems, however, oxides of silicon are routinely found in the pump and exhaust components. This is unexpected and suggests that a counterflow transport mechanism is responsible for conveying air and other contaminants up-stream toward the pump.

All dry vacuum pumps generate pressure fluctuations in their exhaust pipes. We propose that these approximately sinusoidal pressure waves produce a near-wall system of stable vortices which efficiently transport gas counter to the normal flow in the exhaust system. We also propose that this

 0734-211X/94/12(4)/2763/5/$1.00

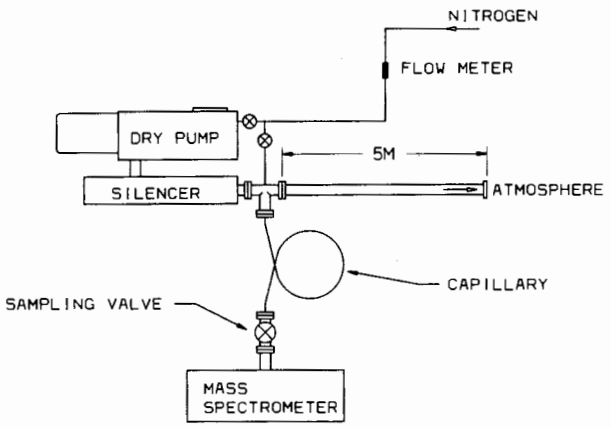

FIG. 1. Experimental setup. The 40 mm diam exhaust line was made of 1 m sections of stainless-steel pipe open to the atmosphere at one end. The sampling capillary tube was 0.5 m long and 0.5 mm i.d.

transport mechanism arises from a phenomenon known as Richardson's annular effect.[2–4]

II. EXPERIMENTAL RESULTS AND DISCUSSION

In attempting to explain the presence of silicon oxides near the exhaust port of an operating process pump, experiments were first carried out with the pump switched off and with process-typical mixtures of dichlorosilane, ammonia, and nitrogen flowing directly into the exhaust line—no oxides were found although other chemical compounds were generated. This was done to eliminate the possibility that residual oxygen contamination in the nitrogen supply might be the cause of the oxide deposits, but many process tools and pumps use very pure nitrogen, yet oxides are still observed.

It was thought that the oxides might be generated during periods of process tool shutdown, when air can migrate back up the exhaust pipe and react with one or more of the compounds already deposited in the exhaust system. In the semiconductor industry, it is routine to place equipment in a standby condition for maintenance; the system is shut down in a controlled manner, leaving all of the pumping system filled with dry nitrogen at atmospheric pressure. However, chemical analysis of the deposits from the exhaust systems of process tools which run for extended periods without shutdown has shown that substantial quantities of oxide are already incorporated into the material.

Having ruled out these possible causes of oxide formation, a systematic study of the behavior of the gases in the exhaust pipe was then undertaken.

Experiments were performed first under quasistatic conditions to establish whether convection might be responsible for the counterflow transport of air. This could best be checked by measuring how closely the oxygen transport approached the limiting conditions for interdiffusion. The quasistatic conditions were then perturbed by imposing a pressure pulsation from the exhaust stage of a pump.

The experimental setup is shown schematically in Fig. 1. It consisted of an 80 m^3/h dry pump fitted with an efficient exhaust silencer, and with a 40 mm diam exhaust line made of 1 m sections of stainless-steel pipe which was open to the atmosphere at one end. The pump was blanked off at the input, resulting in zero net throughput. The gas composition was analyzed with a VG SPX 600 mass spectrometer connected to the exhaust line, immediately after the silencer, via a capillary tube and leak valve. Commercial-grade nitrogen (99.9%) was introduced through a flow meter either to various points on the pump or to the exhaust line. The time constant of the mass spectrometer sampling system, determined for each experiment, was typically in the range 6–10 min.

In order to establish a limit for the rate of back migration of air under quasistatic conditions, experiments were carried out with the pump inoperative and valved off from the exhaust line. The pipeline was thoroughly purged with nitrogen until the oxygen partial pressure was lower than 0.2 mbar—this partial pressure was the base-line pressure for all subsequent measurements. The nitrogen flow was then stopped and residual gas analyzer (RGA) measurements were begun as a function of time for various pipe lengths and orientations.

For measurements on static columns of nitrogen, the throughput of the sampling system was 5×10^{-3} mbar ℓ/s (1.8×10^{-2} sℓ/h), extracted from a pipe volume of 1.26 ℓ per 1 m sections of pipe. *The total amount of gas extracted by the sampling system can be significant over the time scale of an interdiffusion experiment.* For instance, for a 5 m pipe of volume 6 ℓ, the sampling system could remove 2.5 standard ℓ in 132 h, the theoretical time taken for the oxygen partial pressure to increase from 0% to 50% of its atmospheric value due to interdiffusion alone. This problem was insignificant within the time scale taken to achieve 10% or less of atmospheric concentration, but caused large errors for higher concentrations.

A different procedure was used to measure the backmigration effect with the pump in operation. With the pump running, nitrogen was introduced into the pump at a flow rate of 50 ℓ/min for 1 h, after which the flow was switched off and the RGA measurements were begun. Since the appearance of the air signature was very rapid in this mode, the sampling response time was decreased by short periods of pumping the capillary (immediately before the sampling valve) with an auxiliary rotary pump. This reduced the time constant of the sampling system to less than 2 min.

To assess acoustic standing waves as a mechanism for air counterflow, a section of the pipe was replaced with a 1 m glass tube of the same diameter, into which a small amount of ultrafine silica dust could be introduced. The dust tended to stay suspended in the pulsating gas column until it became electrostatically charged, whereupon the next encounter with the glass wall caused it to adhere to the glass. The resulting powder patterns are shown in Fig. 2, where it can be seen that the axial structure has a characteristic dimension of order 3–4 mm. The excitation spectrum was determined by means of a wide bandwidth pressure sensor attached to the exhaust pipe. Since the mechanism of the vacuum pump rotated at 50 Hz with one exhaust discharge per revolution, most of the pressure energy was contained in the 50 Hz

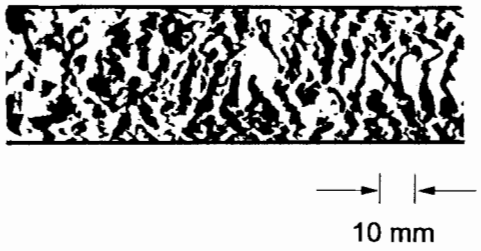

FIG. 2. Silica dust deposition pattern in a 1 m glass tube of 40 mm diam. The axial structure has a characteristic dimension of order 3–4 mm.

fundamental. The next most significant band was the 600–1600 Hz range which corresponds mainly to harmonics generated by high velocity gas flows through the ports of the pump. There was very little energy above 1600 Hz. Standing waves would exhibit structure of characteristic dimension greater than 100 mm for the observed energy distribution and were therefore discounted.

Figure 3 shows results for air, measured under quasistatic conditions using a horizontal, 5 m length of pipe. An oxygen signal began to appear after 5 h and increased steadily over the next 28 h after which the experiment was terminated because of the sampling effect. It can be seen that the results were a factor 2.5 removed from the theoretical curve, suggesting that some mechanism other than interdiffusion was assisting the transport. It is probable that, over such extended time scales, free convection was playing a role. This was checked by measurements using shorter lengths of pipe in different orientations, with some evidence that orientation affected the migration rate. These experiments were difficult to control and gave results with wide scatter. However, the oxygen concentration always increased significantly faster than predicted for interdiffusion.

Also shown in Fig. 3 are results obtained for the same arrangement but with the pump switched on. The oxygen

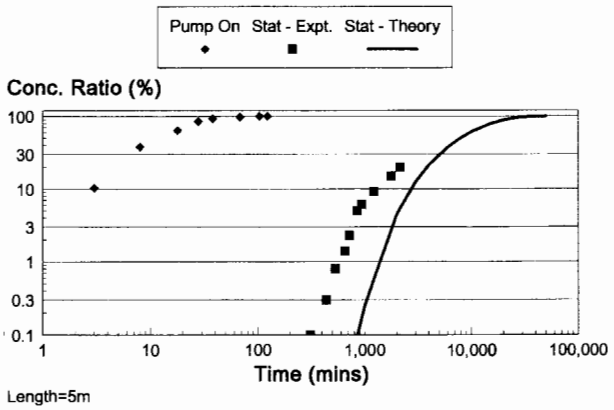

FIG. 3. Concentration of oxygen at the sampling point in the exhaust line as a function of time. (a) The calculated oxygen concentration due to static interdiffusion along a 5 m pipe for $D_{12}=0.2$ cm^2/s. (b) Experimental results for diffusion in a 5 m horizontal column of nitrogen at 22 °C. The shift of the experimental curve is attributed to convection effects. (c) The measured oxygen concentration due to a 50 Hz pulsation in the nitrogen column, with no N_2 flow.

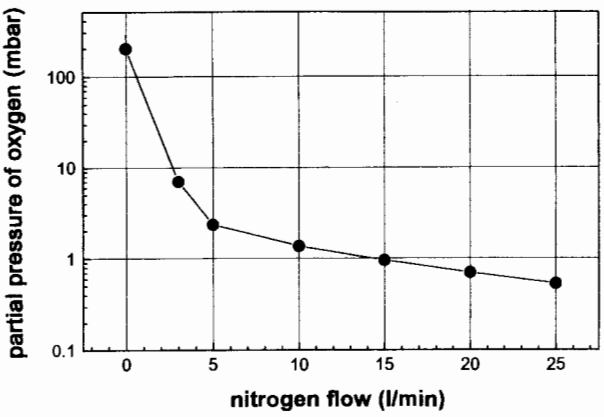

FIG. 4. Variation of the equilibrium partial pressure of oxygen at the sample point (pump on) as a function of nitrogen purge flow. For N_2 flow rates greater than 5 ℓ/min, the concentration falls approximately as 1/(flow rate).

signal appeared too quickly to be resolved by the sampling system and increased to 64% of atmospheric concentration (assumed to be 200 mbar partial pressure in all experiments) in only 18 min. This was more than 2 orders of magnitude faster than for convection/interdiffusion.

The influence of a normal flow of nitrogen (introduced into the pump) on the observed backmigration effect was determined for several flow rates and is shown in Fig. 4. A flow rate of 5 ℓ/min reduces the backmigration effect by 2 orders of magnitude but still leaves a partial pressure of oxygen of 2 mbar. The efficiency of the counterflow transport mechanism, even in the presence of significant purge flows of nitrogen, was demonstrated by a simple test: 0.02 sℓ/min of air was injected into the 5 m exhaust system at a point 1.5 m downstream from the silencer, while 0.03 sℓ/min of dichlorosilane and 20 sℓ/min of nitrogen were introduced into the pump. After 24 h, thick deposits (~5 mm) of silicon oxide were found 1 m upstream from the point of air injection. The position of maximum deposition could be varied by changing the nitrogen flow rate, with smaller flow rates moving the deposition zone further upstream (i.e., closer to the pump). This suggests that operation of LPCVD processes with small nitrogen flow rates into the exhaust can result in potentially damaging oxide formation in the exhaust system.

In every experiment carried out with silicon-containing gas and ammonia (or oxygen), the resulting crusts of deposited material exhibit a deeply profiled surface texture which strongly resembles the patterns observed in the dust test using the glass tube. The characteristic dimension in the axial direction of the pattern was ~2 mm.

III. ANALYSIS

A. Interdiffusion under static conditions

In the case of a cylindrical pipe of length L which is long compared to its diameter $2r_0$, the rate of change of concentration at the sample point can be found by solving the one-dimensional diffusion equation

$$\frac{\partial c}{\partial t} = D_{12} \frac{\partial^2 c}{\partial x^2} \quad \text{for } 0<x<L,$$

where D_{12} is the interdiffusion coefficient of the two mixing species and $c(t)$ is the concentration of the "contaminating" species at a distance x from the sample point ($x=0$). Values of D_{12} are given in Dushman[5] for pairs of gases at 0 °C and 1 bar pressure, together with correction factors to compensate for temperature. In this work, a value $D_{12}=0.2$ cm^2/s has been used for O_2–N_2 interdiffusion at 22 °C. A particular solution of the diffusion equation for $c(t)$ at $x=0$ is of the form[6]

$$\frac{c}{c_0} = 1 - \frac{4}{\pi} \sum_{n=0}^{\infty} \frac{(-1)^n}{2n+1} \exp\left(-(2n+1)^2 \pi^2 D_{12} \frac{t}{4L^2} \right),$$

where c_0 is the equilibrium atmospheric concentration of oxygen in air, assumed to be 200 mbar. This expression is plotted in Fig. 3; only the first term in the summation is significant for most considerations. Note that the time to achieve a particular concentration ratio varies as L^2, a result typical of diffusion processes.

B. Richardson's annular effect

For a 40 mm diam pipe at 20 °C, flow will become turbulent when the gas throughput exceeds approximately 770 mbar ℓ/s. For net gas flow rates of order 30 ℓ/min (500 mbar ℓ/s) or less, the flow will be laminar. The pressure drop over a 5 m length of duct will be less than 10^{-2} mbar. The pressure sensor showed that the pressure pulsation in the exhaust pipe after the silencer is approximately sinusoidal and of amplitude up to ±100 mbar. Thus, the pressure gradient in the duct is dominated by the oscillating pressure field and the pressure gradient associated with the mean net flow can be neglected with respect to the oscillating pressure.

Neglecting entrance effects within the duct, the local velocity within the duct is independent of the axial position within the duct and is governed by[7,8]

$$\frac{\partial u}{\partial t} = -\frac{1}{\rho}\frac{\partial P}{\partial x} + \nu\left(\frac{\partial^2 u}{\partial r^2} + \frac{1}{r}\frac{\partial u}{\partial r} \right),$$

where u is the local velocity, r is the radius of the pipe, and ν is the kinematic viscosity. The oscillating pressure driving the flow can be represented by

$$-\frac{\partial P}{\partial x} = \rho K \cos(\omega t),$$

where K is a constant with units of acceleration and ω is the oscillation frequency. Imposing no-slip at the wall and neglecting the start-up transient, the closed form solution for the governing equation is given by

$$u(r,t) = \frac{K}{i\omega} e^{i\omega t}\left(1 - \frac{J_0(r\sqrt{-i\omega/\nu})}{J_0(r_0\sqrt{-i\omega/\nu})} \right),$$

where J_0 is the Bessel function of the first kind, order zero. A dimensionless "kinetic Reynolds number" for the flow can be defined by

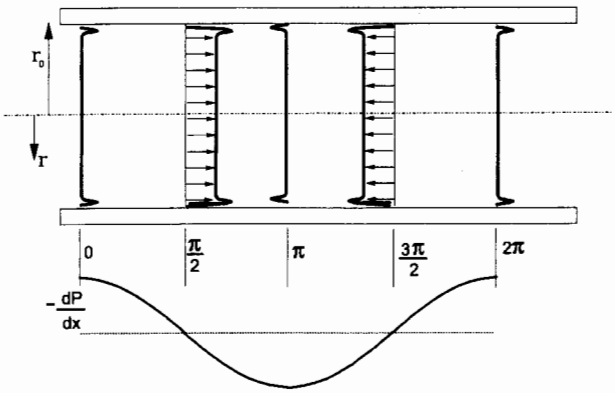

FIG. 5. Instantaneous velocity profiles as a function of oscillation phase and phase shift from driving pressure field. The phase shift is a function of the oscillation frequency and the distance from the wall.

$$\omega^* = \frac{\omega r_0^2}{\nu},$$

which is a measure of inertial forces relative to viscous effects in oscillating flow. For values of $\omega^*>4$, the above closed form solution can be approximated by

$$\frac{u}{u_{\max}} = \frac{4}{\omega^*}\left(\sin(\omega t) - \frac{e^{-B}}{\sqrt{r^*}} \sin(\omega t - B) \right),$$

where

$$r^* = \frac{r}{r_0}, \quad B = (1-r^*)\sqrt{\frac{\omega^*}{2}},$$

and $u_{\max} = Kr_0^2/4\nu$ is a fictitious center-line velocity which would exist for a fully developed Poiseuille flow with pressure gradient $-\rho K$. The velocity u is approximately ±6.7 m/s for the experimental system. An important aspect of the flow field for large ω^* is that the velocity field is out of phase with the pressure field. For very large $\omega^*>2000$, the velocity field lags the pressure field by 90° (Fig. 5) and is very uniform across the entire duct until near to the wall ($r^* \geqslant 0.93$), where the oscillating flows become turbulent and the phase angle changes rapidly. For the experimental situation discussed in this work, ω^* takes values of 7970 at 25 °C and 5400 at 100 °C, i.e., the conditions for turbulence are significantly exceeded.

The low momentum near-wall fluid responds to the changing pressure gradient more quickly than the core fluid. The mean behavior of the velocity field can be further illustrated by the mean square velocity calculated from

$$\overline{u^2}(r) = \frac{\int_0^\tau u^2(r)dt}{\tau},$$

and is shown in Fig. 6; the root-mean-square (rms) velocity overshoot is ~4%. Both the instantaneous velocity profiles and the rms profile exhibit a near wall overshoot with corresponding velocity gradient which changes sign at the local peak velocity. This change in sign of the velocity gradient leads to the presence of two layers of opposite sign vorticity and will enhance mixing between the wall layer and the core

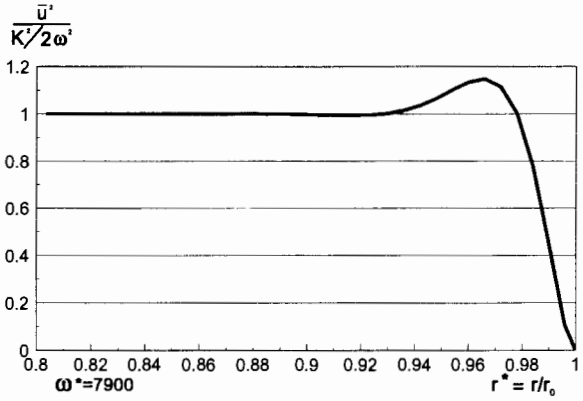

FIG. 6. Near-wall overshoot in velocity profile—Richardson's annular effect.

fluid. Figure 6 predicts a peak velocity at 0.7 mm from the wall and total vortex-affected region of 1.4 mm. Because the flows are turbulent in this region, the dimension of actual vortices can be expected to be somewhat larger.

A probable vortex field structure is shown in Fig. 7 and can be used to account for the counterflow transport of oxygen through the exhaust pipe and the preferential deposition of precipitate in circumferential rings.

During the portion of the oscillation where the fluid is moving upstream toward the pump, oxygen is strongly convected through the core flow region and is mixed into the near-wall vortex layer. During the outward portion of the flow, the near-wall fluid motion is restricted by the no-slip wall condition. During the next in-flow portion of the oscillation, the near-wall fluid containing oxygen from the previous cycle is mixed outward by the reversing sign of the vortices and is moved towards the core flow where it is convected further upstream towards the pump. By this repeating process, oxygen is continuously moved from the core flow to the wall layers and back to the core flow, establishing a much stronger transport than would exist due to diffusion alone. As oxygen mixes with excess reactants, a precipitate forms and becomes trapped in the low momentum near-wall vortex layers. Close to the wall where the fluid momentum is not sufficient to transport the solid particles, the precipitate deposits preferentially between adjacent vortices. The presence of the particles on the wall probably also results in preferential location (or pinning) of vortex cells and reinforces their structure. Also, in locations where vortices have become pinned, it is likely that the very high near-wall shear forces will combine with entrained particle motion to scour loose material from the wall. This is consistent with the deep profiling of deposited crusts found in the exhaust systems of process tools. The characteristic axial dimension of the experimentally observed, circumferential particle deposits is in reasonable agreement with the analytical prediction.

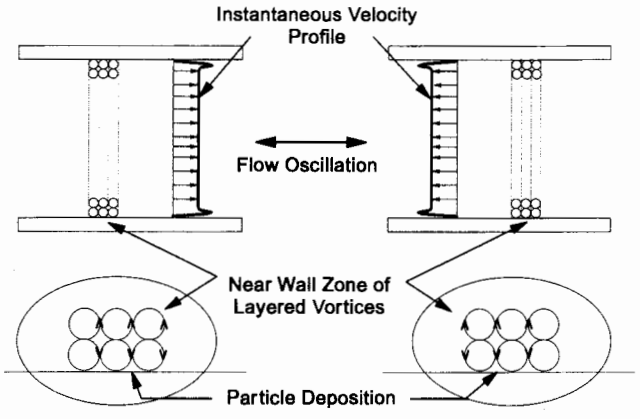

FIG. 7. Proposed near-wall vortex structure produced by high Reynold's number oscillating flow and near-wall velocity overshoot.

IV. CONCLUSIONS

This work has shown that a periodic pressure fluctuation in an exhaust pipe will create a counterflow transport mechanism which can pump gases, against the direction of normal flow, at rates high enough to result in chemical reactions and deposition at (or even in) the pump. The phenomenon can be qualitatively described by Richardson's annular effect. In processes using silane or similar gases, this can lead to unwanted deposition of oxide and other materials which can block the pipeline or damage the pump mechanism. The effect can be reduced by applying a flow of nitrogen but drops off only in rough inverse proportion to flow rate. Even with N_2 flow rates of 20 ℓ/min, there can be thick deposits in the pipe caused by air leaks or by air drawn back from the scrubber or duct. Very low nitrogen flow rates can cause serious problems and the geometry of exhaust lines should be carefully considered to minimize the effect. Low nitrogen flows in gas supply systems to dry pumps can also cause serious problems when process gases and byproducts are transported up the nitrogen supply lines by the pulsations in the vacuum pump.

[1]H. J. Emeleus and K. Stewart, J. Chem. Soc. 1182 (1935).
[2]E. G. Richardson and E. Tyler, Proc. Phys. Soc. London **42**, 1 (1929).
[3]T. Sexl, Z. Phys. **61**, 349 (1930).
[4]S. Uchida and Z. Angew, Math. Phys. **7**, 403 (1956).
[5]S. Dushman, *Scientific Foundations of Vacuum Technique* (Chapman and Hall, London, 1949), p. 76.
[6]H. S. Carslaw and J. C. Jaeger, *Conduction of Heat in Solids* (Clarendon, Oxford, 1959), p. 99.
[7]H. Schlichting, *Boundary Layer Theory* (McGraw-Hill, New York, 1979), p. 408.
[8]F. M. White, *Viscous Fluid Flow* (McGraw-Hill, New York, 1991), p. 100.